Construction and Building Materials 148 (2017) 887–899

Contents lists available at ScienceDirect

Construction and Building Materials

journal homepage: www.elsevier.com/locate/conbuildmat

Influence of the sheet profile design on the composite action of slabs made of lightweight woodchip concrete

Danièle Waldmann *, Andreas May, Vishojit Bahadur Thapa

Laboratory of Solid Structures, University of Luxembourg, Luxembourg

HIGHLIGHTS

- Analysis of the load-bearing capacity of composite slabs using lightweight woodchip concrete.
- Lightweight woodchip concrete ensured a dead load reduction of 50% compared to normal concrete.
- The shape of the profiled steel sheeting has a significant impact on the load-bearing capacity.
- All specimens presented a ductile bond behaviour over the whole bond length.
- Lightweight woodchip concrete is applicable in steel-composite slab systems.

ARTICLE INFO

Article history:
Received 16 September 2016
Received in revised form 26 April 2017
Accepted 28 April 2017

Keywords:
Composite slab
Profiled steel sheeting
Lightweight concrete
Woodchip aggregates

ABSTRACT

The trend for using renewable materials in construction to create sustainable and robust buildings is currently gaining in popularity. Therefore, in this work, the applicability of dense lightweight woodchip concrete in constructive engineering is investigated. Here, the material is used as a top concrete layer on composite floors with profiled sheets and is analysed with regard to its load-bearing behaviour and composite action. One specific concrete mixture which fulfils the requirement for minimum strength of LC 20/22 is used for the test series. The scale of the study comprises 22 plate elements in total. The varied parameters are the shear spans, profiled sheet types and sheet thicknesses. Each examined sheet has an undercut profile with additional embossment. On the basis of experimental results, the influences of the varied parameters and profile forms on the load-bearing and composite behaviour are discussed. This study provides important key findings which show that dense lightweight woodchip concrete can transfer sufficient longitudinal shear forces to the composite joint.

1. Introduction

Today's owners show greater interest in data on energy, ecology and health of new constructions or renovations. In contrast to what have been hitherto predominantly investment-oriented considerations, emphasis is now increasingly laid on the complete life cycle of buildings. Building materials made out of renewable resources can make a significant contribution to saving limited fossil energy resources and reducing additional CO_2 emissions. While porous lightweight woodchip concrete is already applied as sound-absorbing materials and insulation materials, the questions that arise now are whether dense lightweight woodchip concrete is applicable as a load-bearing building material and whether existing steel-concrete composite systems are suitable for this kind of concrete.

In particular, the use of steel-concrete composite systems is highly praised in modern construction concepts for buildings and bridges since the coupled structural system takes advantage of the compressive strength of concrete and the high tensile strength of steel in a mixed structure; using steel-concrete composite structures, it is possible to develop highly efficient and high-strength design elements [1–5].

Several experimental tests have been carried out by researchers to investigate the interactions between normal concrete/lightweight concrete and steel sheeting in composite floors [6–17]. Chen [6] reported that for different spans of steel profiled sheeting composite slabs, a longitudinal shear-bond slip was detected and that the slabs with end anchorage bore higher shear-bond strength than those without end anchorage. He concluded that composite slabs were unable to develop full plastic

* Corresponding author.
E-mail address: daniele.waldmann@uni.lu (D. Waldmann).

http://dx.doi.org/10.1016/j.conbuildmat.2017.04.193
0950-0618/

moment in the spans due to shear-bond failure in the steel-concrete contact areas.

In order to study the shear-bond action in embossed composite deck slabs, Marimuthu et al. [7] and Gholamhoseini et al. [11] tested specimens made out of normal concrete and profiled sheets. Their results showed that the failure mode of composite slabs depends on the shear span, as a shear bond failure was found for shorter shear spans whereas a flexural failure was found for larger shear spans. A comparison of the longitudinal shear strength calculated by the m-k method and the partial shear connection (PSC) method showed an average difference of about 26% [7]. Similar results were reported by Hedaoo et al. [8], who carried out bending tests on 18 composite specimens with steel profiled sheeting to investigate the shear bond strength in accordance with Eurocode 4 – Part 1.1 [9]. Mäkeläinen et al. [10] reported that compared to all the different characteristics of embossment, the depth of the embossment has the most effect on shear resistance behaviour. Brunet et al. [12] reported that in contrast to specimens without embossment, specimens with embossments required further slip after the failure of the chemical bond until the maximum shear capacity was achieved. Furthermore, they reported that the bond strength between concrete interface and steel sheets can be considered as a function of the rib geometry rather than an adhesive property because it is predominantly a mechanical property related to the debonding of the interface.

Most of the steel-concrete composite slabs use normal concrete as the concrete top layer; however, more recent studies show great interest in investigating the mechanical behaviour and failure mode of concrete-steel composite decks made of lightweight concrete. Kan et al. [13] performed four-point bending tests on deck specimens made from normal and lightweight concrete and reported that, whether made of normal or lightweight concrete, both steel decks showed similar structural behaviour. Similarly, Luu et al. [14] conducted an experimental investigation on lightweight composite deck slabs made out of lightweight concrete with profiled steel sheeting. The lightweight concrete used for concreting was classified as LC 16/18 and LC 35/38 in accordance with EN 206-1 [15]. Luu et al. reported that the use of lightweight concrete allowed a reduction of the dead load of the composite slab by 40% compared to normal concrete without any loss in structural performance. Penza [16] conducted an experimental study on the longitudinal shear strength of lightweight concrete slabs with trapezoidal steel sheeting. Unlike other investigations [13], she found that the benefit of using lightweight concrete was a 20% reduction in the self-weight, but it caused a loss of load-bearing capacity of 25% for short span slabs and 45% for long span slabs. Furthermore, the specimens with shorter shear span showed better vertical shear capacity and for all the tested slabs, an end slip in the direction of the profiled sheet embossments was found. The results also indicated that the longitudinal shear strength is reduced in comparison to normal concrete.

The application of lightweight wood concrete has increased in recent years and has become the focus of research projects such as [17], where the load-bearing behaviour of slabs made of lightweight woodchip concrete was investigated. The impetus for the work was to use alternative slabs for restructuring older buildings. Lightweight woodchip concrete with a dry bulk density of 1000 kg/m^3 was used. The resulting compressive strengths were of about 5 N/mm^2.

Mostly undercut and trapezoidal profiled sheets with or without mechanical dowelled interface have previously been investigated. For undercut profiled sheets, mechanical interlock develops between the concrete and the profiled steel sheets due to deformation under loading: the bond between both materials is ensured by a mechanical clamping effect when the profiled steel sheets deform. Nevertheless, slippage between both actors will appear due to longitudinal shear stress. Additional embossment of the profiled sheets to prevent slippage is meant to further improve this composite action [18–20,7,21–23,10,24,6,25].

The clamping effect is activated as soon as there is deformation of the undercut sheet under loading and its magnitude is influenced by the loading, the thickness of the profiled sheet and the geometry of the sheets (Fig. 1).

According to [26], for lightweight concrete composite floors, a load drop can be perceived once the ultimate load is reached; in contrast to normal concrete where the ultimate load is retained while bending deformation is increasing. Additionally, crack behaviour is observed which is different to that exhibited by normal concrete composite floors: a main gaping crack failure was established, whereas, for lightweight concrete composite floors, branching crack propagation or even longitudinal cracks were observed.

The main objective of the research was to investigate the usability of a dense lightweight woodchip concrete (Fig. 2, **left**) in structural engineering. Whereas porous lightweight woodchip concrete (Fig. 2, **right**) is already covered by existing standards in terms of its definition, production and assessment of conformity and is used in different engineering applications, investigations on dense lightweight woodchip concrete go no further than determining characteristic material parameters. Therefore, investigations have been performed to determine whether a dense lightweight woodchip concrete fulfils the minimum requirement in terms of strength in the composite with steel profiled sheets with undercut profiles. Furthermore, the load-deflection behaviour, slippage and cracking of two different profiled steel sheeting types are reported showing the impact of embossments as well as their interaction with a less rigid lightweight concrete. It is thereby shown that a dense lightweight woodchip concrete generally fulfils the requirements for bonding mechanisms in a composite floor system.

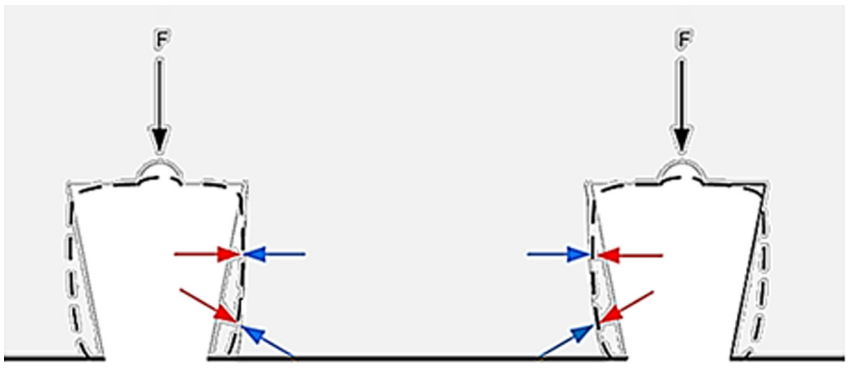

Fig. 1. Clamping effect on the profiled sheet.

Fig. 2. Dense lightweight woodchip concrete (left) and porous lightweight woodchip concrete (right).

2. Test program

2.1. Materials

2.1.1. Type of wood used

The type of wood used for the concrete aggregates was a mixture of spruce and fir. These wood types were added to the concrete mixture in the form of woodchips.

The lignin content of hardwoods is about 18–25%, whereas coniferous woods contain between 28 and 41%. Lignin is a complex organic polymer which is insoluble and hydrophobic. According to Heinz et al. [27], the lignin of wood aggregates has only a minor impact on the hardening of the cement matrix. An additional advantage in using coniferous woods is that they are widespread in the local climate region and being fast-growing can be quickly replenished. Furthermore, coniferous woods are suitable for cement-bound materials because the proportion of monomer sugars, sugar alcohol, lipids and wax is lower than for hardwoods.

The particle size distribution and the particle form of the woodchip aggregates depend on the process in the sawmill production. The fraction size of the used woodchips was 0/8 mm. A classical grain size distribution cannot be established due to bulkiness of the woodchips.

2.1.2. Concrete mixture

The concrete mixture developed for the test series had to fulfil the required minimum strength of LC 20/22 according to EC4-1-1:2004 for the grout topping. The mixture has a water/cement ratio of 0.46 with portion of the cement type CEMI 52.5 N of 600 kg/m^3 and a water content of 275 kg/m^3. Additionally, the coniferous wood content amounted to 85 kg/m^3, the pulverised limestone content to 100 kg/m^3 and the sand content amounted to 508 kg/m^3. The order in which the materials are added is important when preparing lightweight woodchip concrete mixtures so that adhesion of the cement particles to the wooden aggregates is optimized and at the same time, the amount of water absorbed by the woodchips is limited. The mixing process consisted in firstly mixing the coniferous wood, pulverised limestone and sand, next adding the cement and then finally adding water to the mixture to initiate the hardening process.

The tests for hardened concrete were conducted according to DIN EN 12390 [28] and DIN 1048-5 [29]. Table 1 lists the material properties at the age of 28 days.

Both EC 4-1-1:2004 [9] and the certification of the profiled sheets prescribe a minimum strength class for concrete of C 20/25 or LC 20/22. However, as test specifications for a dense lightweight woodchip concrete are not currently available, material strength for the test series was determined according to the specifications for normal concrete and following the specifications for porous woodchip concrete.

Table 1
Results of the strength investigation.

Test 28d*	Component tests	
Cube strength	30.2	[MPa]
Cylinder strength	26.9	[MPa]
Cylinder splitting tensile strength	2.0	[MPa]
Young's modulus	11200	[MPa]
Bending tensile strength	4.6	[MPa]
Bulk density at test state	1.68	[kg/dm^3]
Bulk density, oven-dried	1.37	[kg/dm^3]

* Each result is the mean value of three measurements.

Furthermore, the orientation of the wood fibre influences the characteristics of hardened concrete. Different orientations of the wood fibres have been studied by varying the filling direction of the cylinders. Two different filling directions have been compared: a filling perpendicular to length of the cylinder and a filling parallel to the cylinder length. For the latter, a special casting mould has been created. Table 2 illustrates the results of different tests carried out on cylindrical specimens after a curing time of 28 days.

The change of orientation led to an increase in the cylinder strength of about 3 N/mm^2 corresponding to a percentage increase of 68% and an increase in the Young's modulus of about 85%. This allows the assumption that the anisotropic behaviour of wood is transferred to the lightweight woodchip concrete similar to the increase of strength when loading is applied parallel to the main fibre direction. This behaviour is clearly reflected in the compressive strength, the modulus of elasticity and the tensile strength.

This effect has been taken into account during the production of all the main specimens. This guarantees a dominant fibre orienta-

Table 2
Influence of fibre orientation on the lightweight concrete properties.

Force application across the fibre*	Usual filling of the cylinder perpendicular to the cylinder length [N/mm^2]	Filling of the cylinder parallel to its length [N/mm^2]
Cylinder strength	4.4	7.4
Cylinder splitting tensile strength	0.9	1.1
Young's modulus	2500	4600

* Each result is the mean value of three measurements.

tion parallel to the entire specimen length, so that as the specimen undergoes bending the different woodchips are stressed in the longitudinal axis, and thus act as fibre reinforcement for the concrete.

2.1.3. Material properties of the lightweight mixtures

2.1.3.1. Shrinkage. As the developed concrete mixture is used for load-bearing functions within a composite structure, its deformation behaviour must also be described. However, the deformation behaviour of cement-bound wood materials is characterised by extensive deformation already due to shrinkage resulting from the loss of moisture. Already the deformation without loading due to the loss of moisture during hardening is important as the hardening takes place within the composite situation. The high cement content required to reach a sufficient strength and the hygroscopic characteristics of wood are mainly responsible for this. Fig. 3 shows the strain evolution of a specimen and the variation of relative humidity and temperature over 800 days.

The structure of the wood is responsible for extensive deformation during the swelling and shrinkage process as 90–95% of the cells in coniferous wood are comprised of large, individual hollow sections called tracheid. The moisture content in the wood cells indicates the transition from the swelling to the shrinkage process. At a moisture content of about 60%, the wood cells are waterlogged and maximum swelling can be expected. At a moisture content of about 30%, the fibre saturation point is reached: the internal cell space is empty. Below the fibre saturation point, the water in the cell walls dries and the cell contracts in a tangential direction (shrinkage).

2.1.3.2. Thermal conductivity.

Beside weight reduction, another advantage of lightweight concrete is its reduced thermal conductivity compared to normal concrete. According to DIN 4108-4 [32], the thermal conductivity of normal concrete is 2.1 W/(m*K) and a porous lightweight concrete with a density of 1400 kg/m^3 has a thermal conductivity of around 0.79 W/(m*K). Our investigations into the thermal conductivity of dense lightweight woodchip concrete of the mixture with a density of 1370 kg/m^3 were carried out according to DIN EN 12667:2001 [33] and DIN EN 12939:2001 [34] using the guarded hot plate method. As a result, an average heat conductivity of 0.43 W/(m*K) was achieved. This shows that by adding woodchips as lightweight aggregates, the insulation property of dense lightweight woodchip concrete is about twice as great as that of porous lightweight concrete and four times greater than that of normal concrete. Therefore, dense lightweight woodchip concrete combined with low densities of about 1200–1400 kg/m^3 can be considered as a viable alternative to similar lightweight concrete.

2.1.4. Applied profiled sheets

In the test series, composite profiles with an undercut form including additional mechanical embossments were used exclusively. Two different profiles from different manufacturers were chosen with a profile thickness of 0.75 mm and 1.00 mm respectively. In this paper, these profile sheets are referred to as TYPE A (Fig. 4, **left**) and TYPE B (Fig. 4, **right**).

Both sheets have similar geometries [30,31]:

- Identical widths of about 624 mm
- Identical centric spacing of the upper flange of 150 mm
- Comparable sheet heights: 51 mm (TYPE A) and 56 mm (TYPE B)
- Comparable cross sections of 13.02 cm^2/m and 17.06 cm^2/m for TYPE A and 14.02 cm^2/m and 18.96 cm^2/m for TYPE B (Indication for sheet thicknesses of 0.75 mm and 1.00 mm)

However, these sheets also exhibit differences, mainly in terms of the embossments. Whereas TYPE A only has compact upper flange embossments, those of TYPE B are more elongated and flat. Moreover, the profiling proceeds differently at the flanks of the webs. The TYPE B profile sheets also have lateral embossments on the webs.

Using these profiled sheets that appear at first glance to be almost identical, it is possible to demonstrate the influence of embossment on the mechanical interactions of these kinds of profiled sheets with a less rigid lightweight woodchip concrete.

2.1.5. Assessment of the performance of woodchip composites

Table 3 shows the maximum load resulting from a 3-point bending test performed according to [28] on specimens of 1.1 m in length, a width of 45 cm and a height of 16 cm with and without profiled steel sheeting. The profiled steel sheet used for the specimens was of TYPE A. The corresponding self-weight and maximum load were calculated for a specimen of the same dimensions by using the properties of a normal concrete C30/37 according to [15].

Compared to normal concrete classified as C20/25 in accordance with [15], the use of lightweight woodchip concrete made it possible to reduce the dead load of the structure by about 48%, but resulted in a loss of about 20% in structural performances. Compared to the findings of Penza [16], the composite elements studied presented a higher reduction of self-weight.

Furthermore, Table 3 also indicates that the profiled steel sheeting only contributes to a slight increase in the self-weight of the specimen. However, the use of lightweight woodchip concrete with profiled steel sheeting is high-performing in terms of structural performance as it can bear approximately four times more flexural load than lightweight woodchip concrete without profiled

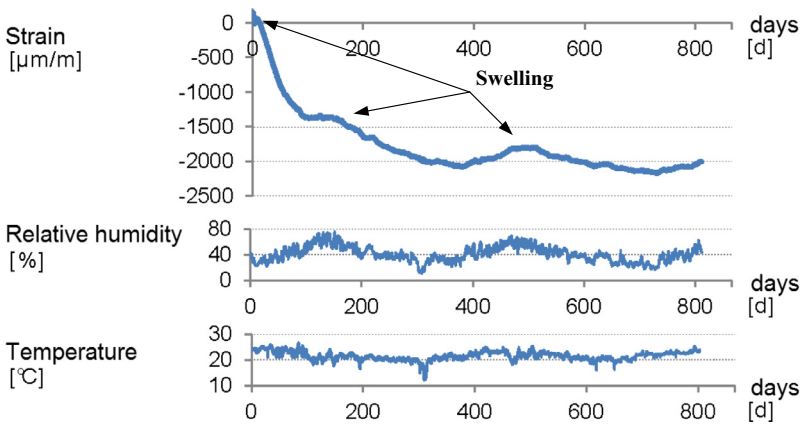

Fig. 3. Strain development of lightweight woodchip concrete; relative humidity and temperature over 800 days.

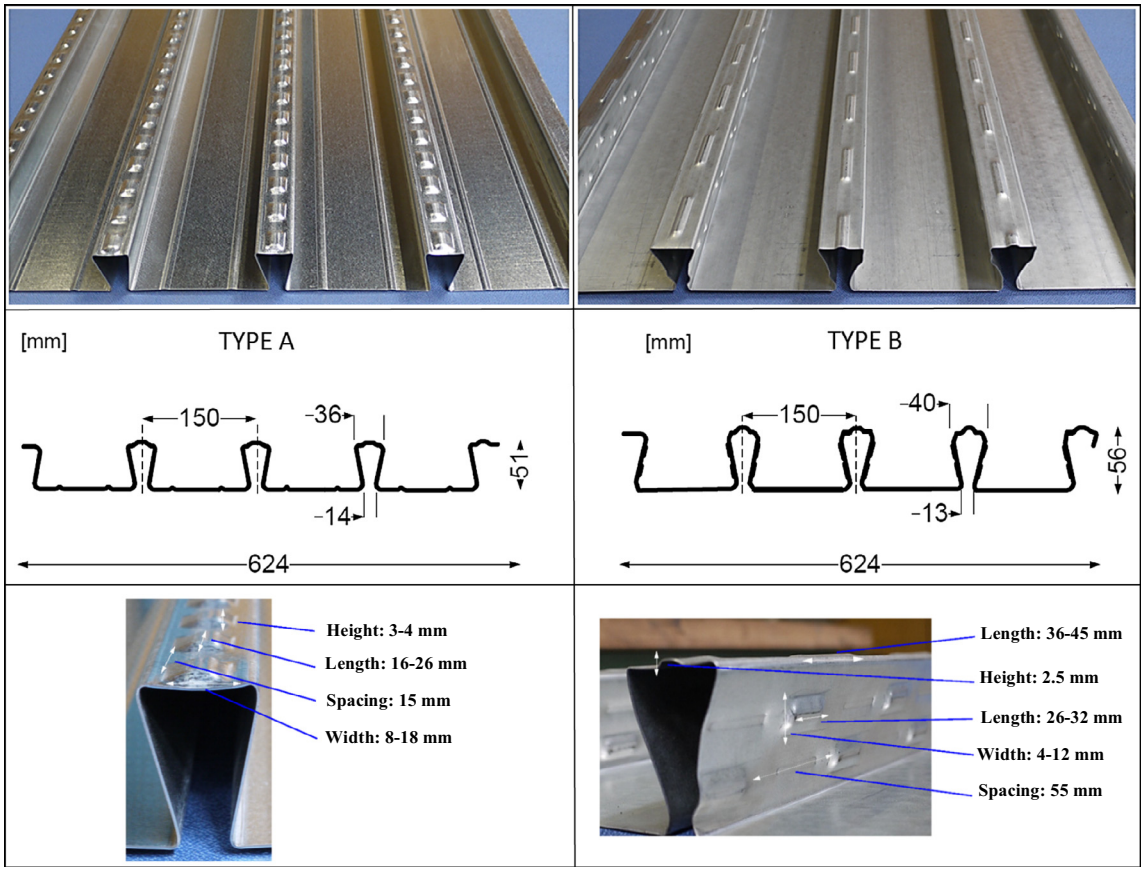

Fig. 4. Applied profiled sheets, dimensions of the profiled sheets and spacing and dimensions of the embossments for TYPE A profiled sheet (left) and TYPE B profiled sheet (right).

Table 3
Self-weight and maximum load capacity of lightweight woodchip concrete with or without profiled steel sheeting and normal concrete.

Lightweight woodchip concrete*	Self-weight [kg]	Maximum Load [kN]
Without profiled steel sheeting	106.9	23.3
With profiled steel sheeting of TYPE A	114.3	106.3
*Each result is the mean value of three measurements		
Normal concrete according to [15]	Self-weight [kg]	Maximum Load [kg]
Normal concrete C20/25	205.9	28.9

steel sheeting and three times more load than normal concrete of class C20/25. These advantageous characteristics of the steel-concrete composite means it is possible to achieve lower construction loads and higher structural performances with a lighter and ecological composite design.

2.2. Experimental setup and procedure

The experimental setup was configured according to the guidelines of EC 4-1-1:2004 Annex B.3 [9], which regulate the experimental procedure and requirements regarding plate dimensioning. This examination included four experimental series which were differentiated by the embossment of the two different types of profiled sheets as well as their thickness of 0.75 mm and 1.0 mm. Each test series included four test specimens with a longer shear span (1.0 m) and one specimen with a shorter shear span (0.6 m). The actual plate length was defined according to the shear span L_{sf}. The shear span is hereby defined as the distance between the load application and the support (Fig. 5).

In total, the examination comprised 22 test specimens which were divided into four test series (Table 4) and two additional elements to illustrate the influence of the component height.

Moreover, crack initiation sheets were mounted which allow the shear span to be precisely defined (Fig. 6).

The experimental setup is compliant with the guidelines of EC 4-1-1:2004 Annex B.3 [9], which predetermines the type of loading, the position of load application as well as the support widths and the protrusion of the slab at the supports. The experimental setup is illustrated schematically in Fig. 7 **(left)**. Fig. 7 **(right)** shows the significant deformability of the test specimen before the ultimate limit state is reached.

2.2.1. Applied measuring techniques

After the setup was prepared, it was equipped with displacement transducers which were distributed horizontally and vertically. Three vertical displacement transducers recorded deflections in the middle of the plate and below the load application. The horizontal displacement transducers documented deformations due to slippage at the end surfaces of the plates by recording the relative displacements between the concrete and the profiled sheets (Fig. 7). In addition, two force transducers were installed at the load application points.

2.2.2. Experimental procedure

The loading of the components was conducted as prescribed in EC 4-1-1:2004 [9] until the failure of the test body occurs at least one hour after loading. The drive of the press for all test series

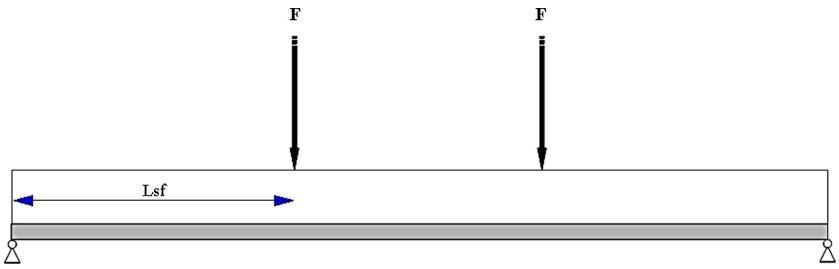

Fig. 5. Definition of the shear span L_{sf}.

Table 4
Overview of the test series.

Type	Profiled sheet thickness [mm]	Element height [cm]	Shear span [cm]	Sample ID	Loading type
TYPE A	0.75	18	100	I-01-LS-0.75-TYPE A	static
				I-02-LZ-0.75-TYPE A	cyclic
				I-03-LZ-0.75-TYPE A	cyclic
				I-04-LZ-0.75-TYPE A	cyclic
			60	I-05-KS-0.75-TYPE A	static
	1.00	18	100	II-06-LS-1.00-TYPE A	static
				II-07-LZ-1.00-TYPE A	cyclic
				II-08-LZ-1.00-TYPE A	cyclic
				II-09-LZ-1.00-TYPE A	cyclic
			60	II-10-KS-1.00-TYPE A	static
TYPE B	0.75	18	100	III-11-LS-0.75-TYPE B	static
				III-12-LZ-0.75-TYPE B	cyclic
				III-13-LZ-0.75-TYPE B	cyclic
				III-14-LZ-0.75-TYPE B	cyclic
			60	III-15-KS-0.75-TYPE B	static
	1.00	18	100	IV-16-LS-1.00-TYPE B	static
				IV-17-LZ-1.00-TYPE B	cyclic
				IV-18-LZ-1.00-TYPE B	cyclic
				IV-19-LZ-1.00-TYPE B	cyclic
			60	IV-20-KS-1.00-TYPE B	static
TYPE A	0.75	15	60	I-21-KS-0.75-TYPE A	static
		12		I-22-KS-0.75-TYPE A	static

Explanation of the sample identifier:

Test series:	I–IV
Plate number:	01–20
Shear span:	K (short) or L (long)
Type of loading:	S (static) or Z (cyclic)
Sheet thickness:	0.75 mm or 1.00 mm
Sheet profile:	TYPE A or TYPE B

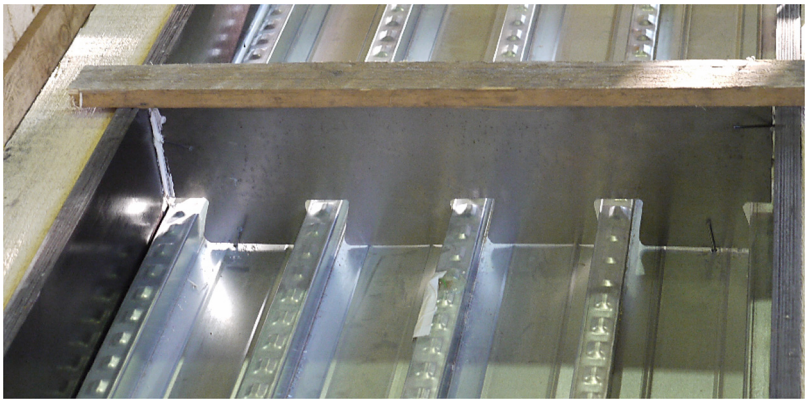

Fig. 6. Crack initiation sheets before casting.

was path-controlled and the loading of the plates was carried out statically or with a combination of cyclic and static loading.

2.2.2.1. Static loading. Static loading was applied to the plates with short and long shear spans. The chosen load speed was 12.5 mm/h and the load was applied in load steps respecting a holding period of 30 minutes each until the load-bearing capacity was reached. The first load step began at a load of 12.5 kN and was increased in steps of 7.5 kN. When slippage occurred, the load increase was changed to 5 kN.

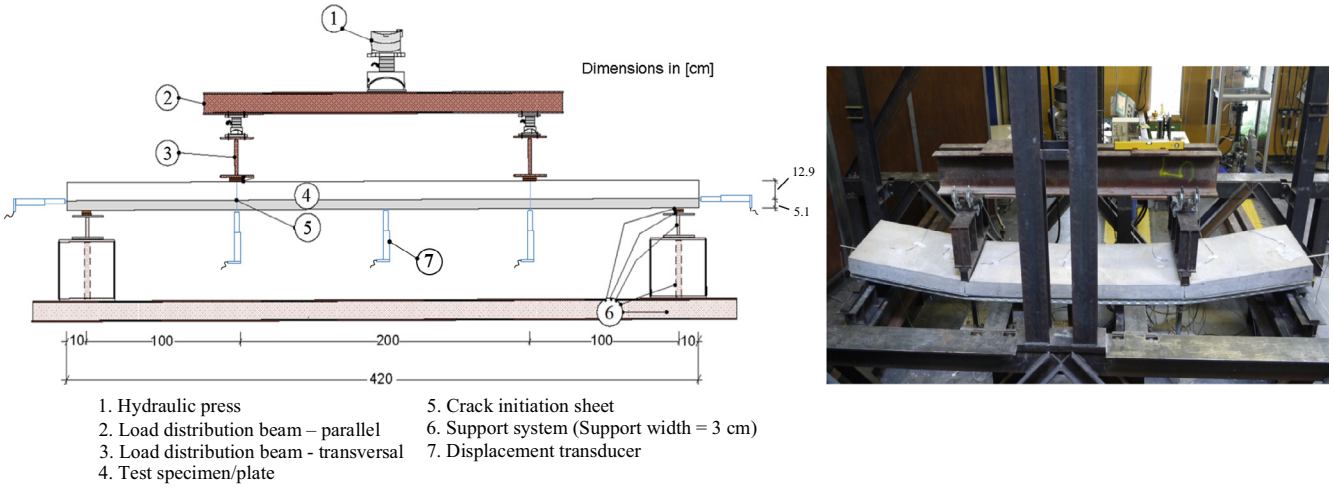

Fig. 7. Scheme of the experimental setup (left) and the specimen under large deflections (IV-18-LZ-1.00-TYPE B) (right).

2.2.2.2. Cyclic loading. According to EC 4-1-1:2004 [9], a cyclic preload of 5000 load alternations within three hours is prescribed. This corresponds to a frequency of 0.46 Hz. This investigates the fatigue behaviour of the components which represents a particular load for the lightweight concrete under consideration. For the cyclically tested plates, the static load steps of 5 kN were only applied after the load cycle of 5000 load alternations. Fig. 8 shows a general model of the load deflection curves of the cyclic tests.

3. Test results

The different component tests were assessed in terms of load-bearing behaviour, bond properties and crack propagation properties. This assessment should illustrate the influence of the stiffness of the profiled sheet (0.75 mm and 1.00 mm) and the type of sheet (TYPE A and TYPE B) in combination with the dense woodchip concrete on the structural behaviour. In addition, the experimental results for both sheet types were compared and analysed with regard to the composite effect.

3.1. Results of the load tests

The static test results are summarized in Table 5 and the results of the dynamic tests are presented in Table 6**.** All test specimens presented ductile bond behaviour over the whole bond length. The load-slip behaviour of all specimens showed that after a decrease at first slip, the loading could still be considerably increased. Specimens with profiled sheets of TYPE A showed an

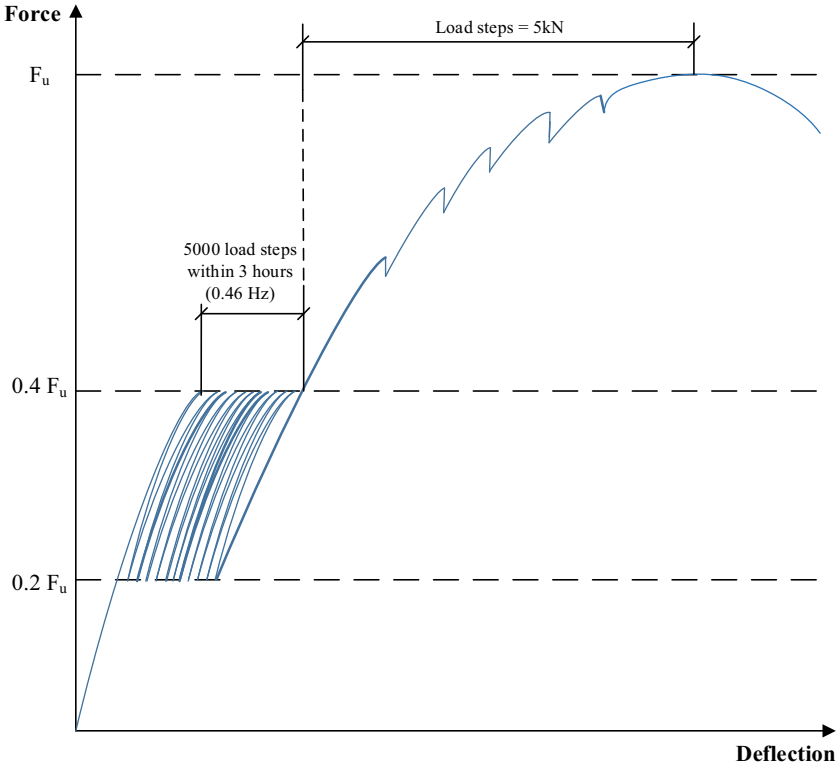

Fig. 8. General illustration of the load deflection curve of the cyclic tests.

Table 5
Summary of the static test results.

Type	Sample ID	Ultimate load [kN]	Deflection at ultimate load mid span [mm]	First slip [kN]
TYPE A	I-01-LS-0.75-TYPE A	62.2	79.0	30.1
	I-05-KS-0.75-TYPE A	76.2	28.2	37.1
	II-06-LS-1.00-TYPE A	90.6	98.0	42.6
	II-10-KS-1.00-TYPE A	127.3	49.6	57.8
TYPE B	III-11-LS-0.75-TYPE B	42.3	130.0	24.0
	III-15-KS-0.75-TYPE B	57.8	25.7	37.8
	IV-16-LS-1.00-TYPE B	74.0	155.0	30.5
	IV-20-KS-1.00-TYPE B	100.5	57.2	45.9
TYPE A	I-21-KS-0.75-TYPE A	64.0	42.0	31.0
	I-22-KS-0.75-TYPE A	49.5	47.0	15.0

Table 6
Summary of the cyclic test results.

Type	Sample ID	Ultimate load [kN]	Deflection at ultimate load mid span [mm]	First slip [kN]
TYPE A	I-02-LZ-0.75-TYPE A	62.6	77.5	22.8
	I-03-LZ-0.75-TYPE A	61.6	75.4	25.0
	I-04-LZ-0.75-TYPE A	60.9	79.5	24.4
	II-07-LZ-1.00-TYPE A	87.8	99.1	32.8
	II-08-LZ-1.00-TYPE A	88.1	97.1	37.0
	II-09-LZ-1.00-TYPE A	88.8	97.0	32.2
TYPE B	III-12-LZ-0.75-TYPE B	39.6	84.5	22.6
	III-13-LZ-0.75-TYPE B	42.9	93.0	24.8
	III-14-LZ-0.75-TYPE B	39.4	92.0	21.2
	IV-17-LZ-1.00-TYPE B	74.9	142.0	32.9
	IV-18-LZ-1.00-TYPE B	73.3	144.0	38.1
	IV-19-LZ-1.00-TYPE B	74.1	132.5	–

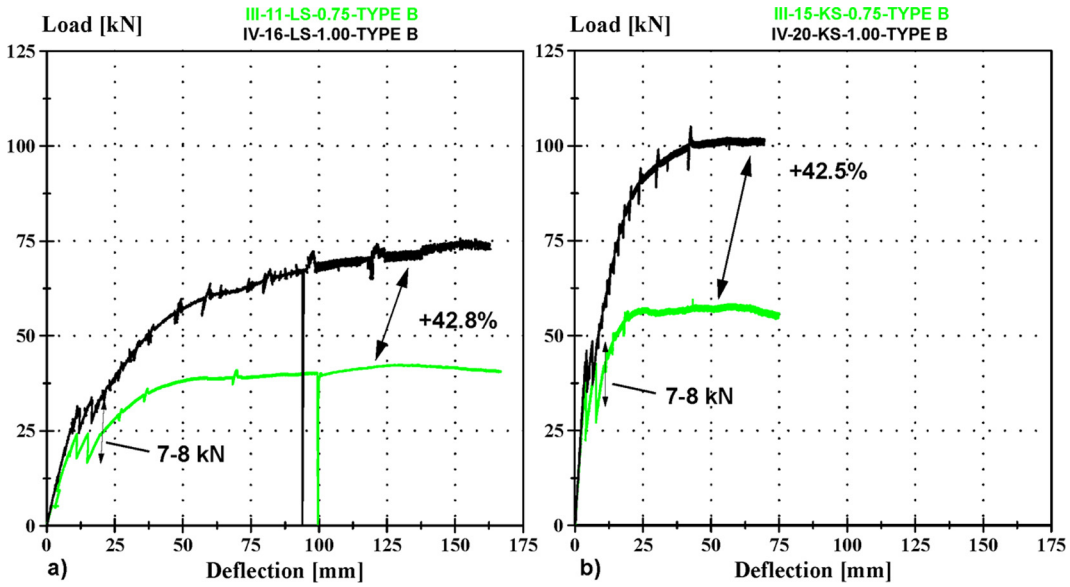

Fig. 9. Comparison of the load course of TYPE B plates; a) long shear span and b) short shear span.

up to 47% higher ultimate load with a deflection at mid-span reduced up to 64% compared to the specimens with profiled sheets of TYPE B. For all specimens, a long shear span led to a reduced ultimate load compared to a short shear span. Furthermore, as expected the profiles with a thickness of 1.0 mm presented a higher ultimate load than those with a thickness of 0.75 mm. They presented a shear bond failure with longitudinal slip after overcoming the chemical bond, the bond due to the clamping effect of the profiled sheet and the slip barrier provided by the embossments. The failure of the specimens will be illustrated in chapter E.

The influence of the examined parameters (Table 4) on load-bearing behaviour is explained in the following sections.

3.1.1. Influence of the thickness of the profiled sheets on load-bearing behaviour

For statically tested plates, an increase in the cross-section of the profiled sheet of about 25% resulted in an increase in the ultimate load of about 43% (Fig. 9). Furthermore, the first slip was observed at a load up to 40% higher for the specimens with profile TYPE A compared to those with profile TYPE B. The load-slip beha-

viour showed for TYPE A specimens that the load could still be increased by more than one time the slip load until reaching the ultimate load, whereas this value was smaller on average for most of the specimens of TYPE B.

3.1.2. Comparison of different types of profiled sheets

In the following, the load deformation behaviour of the two different types of sheet profiles will be compared by using Figs. 10 and 11. Although the cross-sectional area of the TYPE B-profiled sheet is about 7.7% and the moment of area about 34% higher than those for the TYPE A-profiled sheet (Table 7), the load-bearing capacity of the TYPE B-profiled sheet is much lower than that of TYPE A-composite plates. A 22–26% higher load-bearing capacity was found for TYPE A-composite plates with a profile thickness of 1.00 mm compared to TYPE B-composite plates of the same thickness. This difference in load-bearing capacity between both profile types increased to 47% for the composite plates of a profile thickness of 0.75 mm. These differences become clearly visible with the analysis of formation of slippage.

All steel-concrete composite plates present similar stiffness in the initial uncracked state with linear load-deformation behaviour. In the load-deformation diagrams, the formation of slip on the plate sides (release of the adherence bond) can be observed by an abrupt drop in the load before the load rises again due to the activation of the embossment as observed by Kan et al. [13]. When reaching the load where the initial adherence bond has been overcome, increasing deformation results in the formation of a clamping bond between the two composite partners. For the stiffer profiled sheets with increased profile thickness, this occurs at a higher load level than for the profiled sheets with a lower thick-

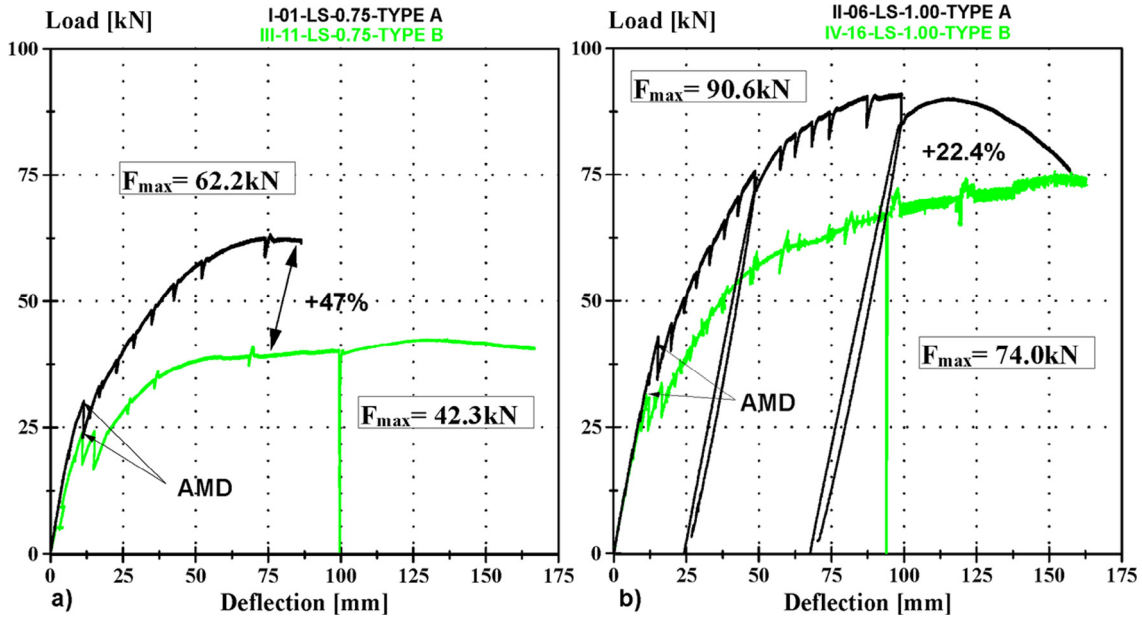

Fig. 10. Comparison of the loads on different sheets with long shear span: a) thickness of 0.75 mm and b) thickness of 1.00 mm.

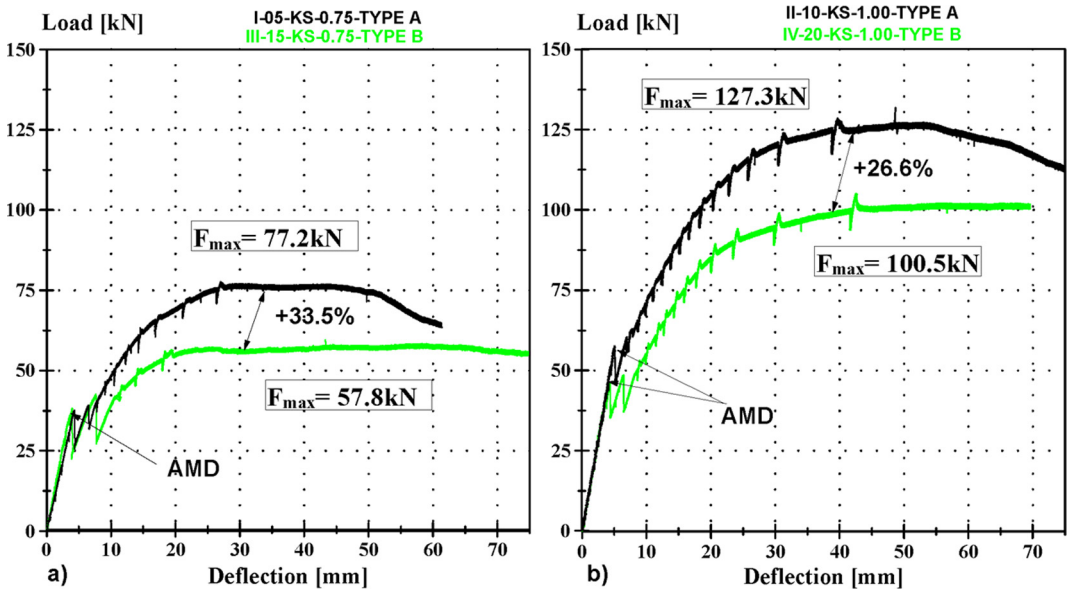

Fig. 11. Comparison of the loads on different sheets with short shear span: a) thickness of 0.75 mm and b) thickness of 1.00 mm.

Table 7
Cross-sectional values of individual test series.

Profiled sheet with thickness	Cross section A_p [cm^2/m]	Moment of inertia I_y [cm^4/m]
TYPE A 1.00 mm	17.60	68.60
TYPE B 1.00 mm	18.96	91.92
Difference in %	7.44	29.05
TYPE A 0.75 mm	13.02	50.70
TYPE B 0.75 mm	14.02	67.99
Difference in %	7.40	29.13

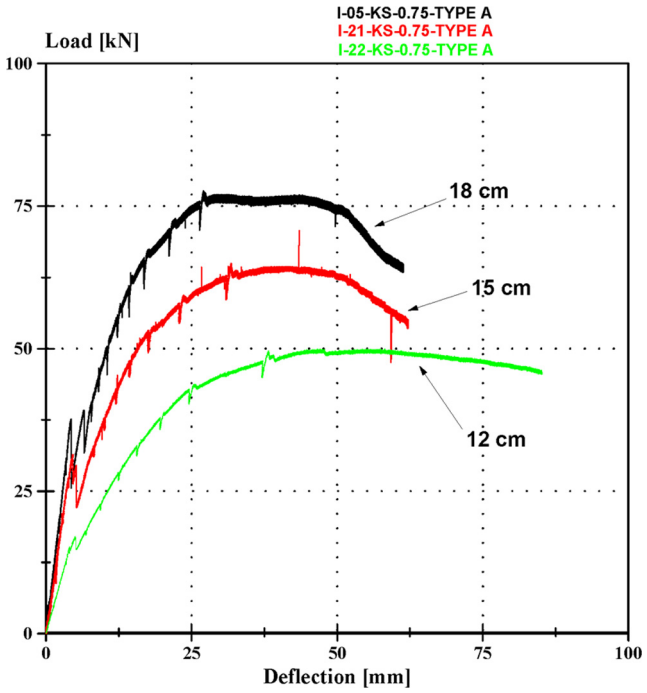

Fig. 12. Influence of the plate height on the load capacity.

ness, and this regardless of profile type. When loading between both types of profiles is further increased, significant differences become apparent. The composite behaviour of the less stiff profile in combination with the lightweight woodchip concrete is considerably better than for the stiffer profile. These observations will be further investigated in subsequent clauses.

3.2. Influence of the height of the component on the load-bearing capacity

Fig. 12 illustrates the different load capacities of three plates with short spans and different heights. The plates have a height of 12, 15 and 18 cm and are of TYPE A with t = 0.75 mm. With increasing plate thickness, the load capacity has increased, as expected, and thereby the respective deflections in the middle of the plate have decreased.

3.3. Interpretation of the composite action

The composite action of different profiled sheets was analysed using the experimental results. The differences for plates with the same profile thicknesses can also be explained using the load-slip diagrams. By way of example, Fig. 13 shows on the statically loaded plates that the TYPE A-composite plates present only small slip deformation both for the thinner and thicker profiles at the load level of slippage, while at this same load level, the TYPE B-composite plates already present a measurable slip of about 1.6–1.9 mm.

The stress marks on the specimens due to the relative displacement between the sheet and concrete at their interface confirm observations from literature. On the one hand, the negatives on the concrete are apparent and on the other, the stress marks on the concrete surface are clearly visible (Fig. 14).

3.4. Influence of the types of profiled sheets on the composite action

In order to investigate the differences between the profile types and their influence on the resulting load-bearing behaviour, the different composite elements were cut open to reveal their cross section and some interesting behaviour was identified.

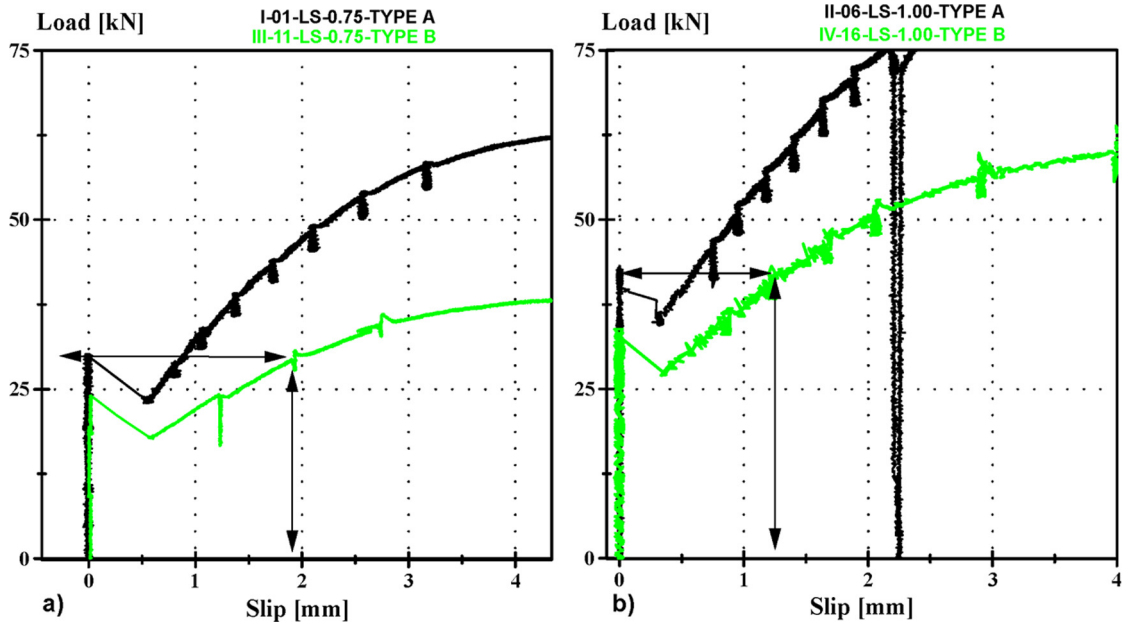

Fig. 13. Example of slip deformation on both types of profiled sheets and both profile thicknesses; a) thickness of 0.75 mm and b) thickness of 1.00 mm.

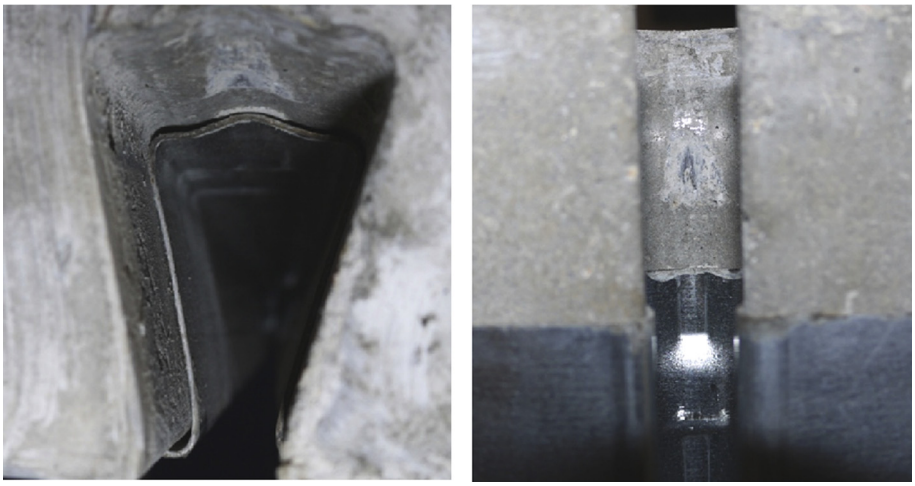

Fig. 14. Stress marks on the lightweight woodchip concrete due to relative displacement (I-04-LZ-0.75-TYPE A).

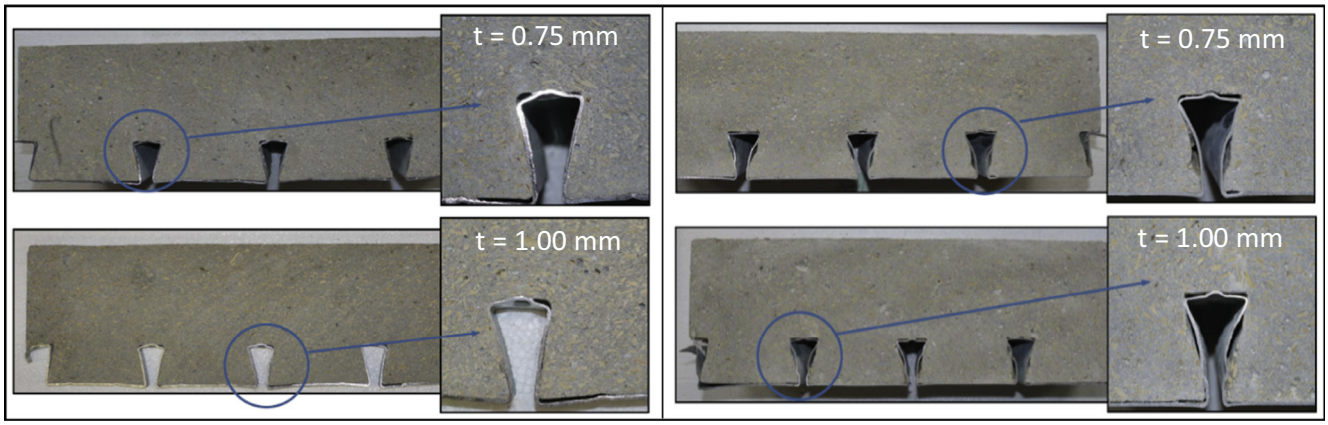

Fig. 15. Cross sections of TYPE A-profiled plates (left) and TYPE B-profiled plates (right) with different profile thickness (t = 0.75 mm and t = 1.00 mm).

Fig. 16. Example of single cracks at the middle of the plate before loading (I-01-LS-0.75-TYPE A).

After the formation of slippage and with the corresponding deformation of the undercut cross section of the profiled sheet, the web surface of the TYPE A profile sheet was pressed laterally against the concrete. Therefore, the contact pressure and the dynamic friction can be entirely transferred to the lightweight woodchip concrete. Fig. 15 **(left)** illustrate the interface which formed due to the deformation of the upper flange of TYPE A-profiled plates.

The situation is different with regard to the TYPE B composite plates (Fig. 15**, right**). As mentioned before, the relative displacement between concrete and profiled sheet compresses the upper flange due to the embossment. In addition, the decisive factor is that the TYPE B profile sheets, as previously stated, also have lateral embossments which are pressed inside the web. This results in the fact that no complete contact can be established at these positions and the contact pressure cannot be entirely transferred, which decreases the clamping effect. Furthermore, local buckling of the lateral profile web is produced.

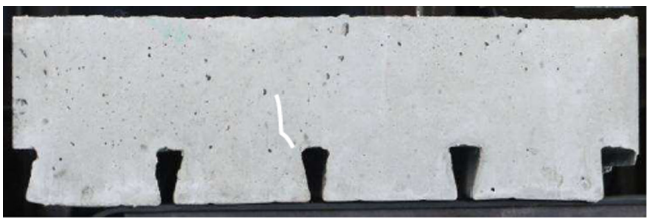

Fig. 17. Example of a geometrically induced single crack (I-01-LS-0.75-TYPE A).

Moreover, the conclusion of Mäkeläinen et al. [10] that the characteristics of the embossments contribute significantly to the shear resistance behaviour was confirmed. As the depth of the embossment is smaller for TYPE B-composite plates (embossment height of 2.5 mm) compared to TYPE A-composite plates (embossment height of 4 mm), more shear stress can be transferred from the lightweight woodchip concrete to the TYPE A profile sheets.

Fig. 18. Example of a geometrically induced single crack (left, III-11-LS-0.75-TYPE B and right, III-15-KS-0.75-TYPE B).

3.5. Analysis of the crack pattern

The failure of all specimens occurred at the load application points due to the insertion of the crack initiation sheets. An analysis of the crack pattern shows that no longitudinal cracks developed on any plate in the various test series. The crack pattern in these test series was limited to the anticipated single bending cracks (without branching) at the cross section of the maximum moment and shear cracks at the point of load introduction and at the supports.

As already stated in chapter II.A.3, the strains due to shrinkage of the lightweight woodchip concrete were more pronounced than those for normal concrete. The test plates were produced without upper transport reinforcement (contraction reinforcement against shrinkage). However, single cracks at the middle of the plates were only detected on a total of five plates out of all test bodies before the start of the experiment (Fig. 16).

These cracks were only observed on edge zones of the concrete surface and did not develop further under loading. On the interface with the profiled sheet, crack formation had already started at geometrically critical spots (internal corners) before the start of the experiment. However, no further propagation of these cracks was observed during loading (Fig. 17).

Few single bending cracks occurred between the load application points. In the shear areas, only one single crack developed which later led to crack formation in the shear area. The following series of pictures documents the crack formation underneath the load application (Fig. 18, **left**). For some components, especially those from the test series with a profile thickness of 1.00 mm, additional diagonal single cracks occurred, but only for high deflections and partly after reaching the load capacity (Fig. 18, **right**).

4. Conclusion

This study presents very promising findings and confirms the benefits of composite structures made of lightweight woodchip concrete and profiled steel sheets for building and construction applications. The key findings from experimental tests on 22 composite specimens are summarized below:

(1) All tested steel-concrete composite plates presented a ductile bond behaviour over the whole bond length as they continued to deform while maintaining their load-bearing capacity. After formation of a first slip, the loading could still be considerably increased up to 2–2.5 times before failure occurred.
(2) The use of lightweight woodchip concrete instead of normal concrete ensured a dead load reduction up to 50%, but also a loss of about 20% in load bearing capacity. The addition of the profiled steel sheeting to the lightweight woodchip concrete contributes to a 7% increase of the self-weight, but increases the load capacity of the composite fourfold.
(3) The significant influence of the thickness of the profiled steel sheets on the applicable ultimate load is verified since an increase in the sheet thickness from 0.75 mm to 1.00 mm corresponding to 25% resulted in a 43% increase in the ultimate load.
(4) Although the cross-sectional area of the TYPE A-profiled sheet is about 7.7% and the moment of area about 34% lower than those for the TYPE B-profiled sheet, the load-bearing capacity of the composite plates with TYPE A-profiled sheet is 22–26% higher for a sheet thickness of 0.75 mm and 47% higher for a sheet thickness of 1.00 mm than those of composite plates with TYPE B profiled sheet.
(5) Overall, TYPE A composite plates presented an up to 40% higher slip load compared to TYPE B composite plates as well as an increase by more than one time the slip load until reaching the ultimate load as the web surface of the TYPE A profile sheet was pressed laterally against the concrete. Therefore, the contact pressure and the dynamic friction can be entirely transferred, which is not the case for the TYPE B profile sheet.
(6) The higher the embossment depth, 4 mm for TYPE A profiled sheet and 2.5 mm for TYPE B profiled sheet, the more shear stress can be transferred from the lightweight woodchip concrete to the profiled sheet.

References

[1] A. Ataei, M.A. Bradford, H. Valipour, Sustainable design of deconstructable steel-concrete composite structures, Proc. Eng. 145 (2016) 1153–1160.
[2] R. Narayanan, Steel-Concrete Composite Structures, Vol. 7, CRC Press, 1988.
[3] R.W. Furlong, Strength of steel-encased concrete beam columns, J. Struct. Div. 93 (5) (1967) 113–124.
[4] J. Qian, Z. Jiang, X. Ji, Behavior of steel tube-reinforced concrete composite walls subjected to high axial force and cyclic loading, Eng. Struct. 36 (2012) 173–184.
[5] N.E. Shanmugam, B. Lakshmi, State of the art report on steel–concrete composite columns, J. Constr. Steel Res. 57 (10) (2001) 1041–1080.
[6] S. Chen, Load carrying capacity of composite slabs with various end constraints, J. Constr. Steel Res. 59 (3) (2003) 385–403.
[7] V. Marimuthu, S. Seetharaman, S.A. Jayachandran, A. Chellappan, T.K. Bandyopadhyay, D. Dutta, Experimental studies on composite deck slabs to determine the shear-bond characteristic (m–k) values of the embossed profiled sheet, J. Constr. Steel Res. 63 (6) (2007) 791–803.
[8] N.A. Hedaoo, L.M. Gupta, G.N. Ronghe, Design of composite slabs with profiled steel decking: a comparison between experimental and analytical studies, Int. J. Adv. Struct. Eng. (IJASE) 4 (1) (2012) 1–15.
[9] EN 1994-1-1, Eurocode 4: design of composite steel and concrete structures. Part 1. 1: general rules and rules for buildings, European Committee for Standardization, Brussels, 2004.

[10] P. Mäkeläinen, Y. Sun, The longitudinal shear behaviour of a new steel sheeting profile for composite floor slabs, J. Constr. Steel Res. 49 (2) (1999) 117–128.
[11] A. Gholamhoseini, R.I. Gilbert, M.A. Bradford, Z.T. Chang, Longitudinal shear stress and bond–slip relationships in composite concrete slabs, Eng. Struct. 69 (2014) 37–48.
[12] M.J. Burnet, D.J. Oehlers, Rib shear connectors in composite profiled slabs, J. Constr. Steel Res. 57 (12) (2001) 1267–1287.
[13] Y.C. Kan, L.H. Chen, T. Yen, Mechanical behavior of lightweight concrete steel deck, Constr. Build. Mater. 42 (2013) 78–86.
[14] T. Luu, E. Bortolotti, B. Parmentier, X. Kestemont, M. Briot, J.C. Grass, Experimental investigation of lightweight composite deck slabs. In Proceedings of the 9th International Conference on Steel Concrete Composite and Hybrid Structures, 2009.
[15] EN 206-1-2000. Concrete – Part 1: Specification, performance, production and conformity.
[16] A. Penza, Composite slabs with lightweight concrete: experimental evaluation of steel decking and lightweight concrete Doctoral Thesis, Politecnico di Milano, 2010.
[17] K. Schernberger, Holzspanbeton-Verbunddecken: Übersicht bestehender Ansätze sowie Entwicklung und Versuche mit handelsüblichen Holzspänen. Diploma thesis at TU Wien, 2011.
[18] B.S. Mohammed, M.A. Al-Ganad, M. Abdullahi, Analytical and experimental studies on composite slabs utilising palm oil clinker concrete, Constr. Build. Mater. 25 (8) (2011) 3550–3560.
[19] M. Ferrer, F. Marimon, M. Crisinel, Designing cold-formed steel sheets for composite slabs: an experimentally validated FEM approach to slip failure mechanics, Thin-walled Struct. 44 (12) (2006) 1261–1271.
[20] S.A. de Andrade, P.C.D.S. Vellasco, J.G.S. da Silva, T.H. Takey, Standardized composite slab systems for building constructions, J. Constr. Steel Res. 60 (3) (2004) 493–524.
[21] T. Faust, Lightweight Concrete in Composite Structures, Institut fur Massivbau und Baustofftechnologie, Universitat Leipzig, LACER, 1997, p. 2.
[22] M. Crisinel, F. Marimon, A new simplified method for the design of composite slabs, J. Constr. Steel Res. 60 (3) (2004) 481–491.
[23] P.W. Harding, The Development of Composite Flooring Systems Research Report, Cardiff University College, 1986.
[24] G.M. Ganesh, A. Upadhyay, S.K. Kaushik, Simplified design of composite slabs using slip block test, J. Adv. Concr. Technol. 3 (3) (2005) 403–412.
[25] P. Vainiūnas, J. Valivonis, G. Marčiukaitis, B. Jonaitis, Analysis of longitudinal shear behaviour for composite steel and concrete slabs, J. Constr. Steel Res. 62 (12) (2006) 1264–1269.
[26] W. Kurz, V. Mechterine, A. Brüdern, S. Hartmeyer, C. Kessler, Leicht Bauen mit Verbunddecken im Wohnungs- und Gewerbebau, Fraunhofer IRB Verlag, 2009.
[27] D. Heinz, L. Urbonas, Holzbau der Zukunft. Teilprojekt 16. Reihe Holzbauforschung, Fraunhofner IRB Verlag, 2008.
[28] DIN EN 12390: Testing hardened concrete – Part 1: Shape, dimensions and other requirements for specimens and moulds; German version EN 12390–1:2012.
[29] DIN 1048–5:1991, Prüfverfahren für Beton- Teil 5: Festbeton gesondert hergestellter Probekörper, Deutsches Institut für Normung e.V., Beuth Verlag GmbH, Berlin.
[30] Swiss Panel SP44S, Zulassungsbescheid T11–180, Stahltrapezprofile, Fa. Montana Bausysteme AG, Landesdirektion Leipzig, Landesstelle für Baustatik, Leipzig 2006.
[31] Type Brastra-Verbunddecken, Zulassungsbescheid Z-26.1-22, Type Brastra 40 und 70 Verbunddecke, Arcelor Bauteile GmbH Deutschland, Deutsches Institut für Bautechnik 2007.
[32] DIN 4108–4:2013–02, Wärmeschutz und Energie-Einsparung in Gebäuden - Teil 4: Wärme- und feuchteschutztechnische Bemessungswerte. English: Thermal insulation and energy economy in buildings - Part 4: Hygrothermal design values.
[33] DIN EN 12667:2001–05, Thermal performance of building materials and products - Determination of thermal resistance by means of guarded hot plate and heat flow meter methods - Products of high and medium thermal resistance, German version of EN 12667:2001.
[34] DIN EN 12939:2001–02, Thermal performance of building materials and products - Determination of thermal resistance by means of guarded hot plate and heat flow meter methods - Thick products of high and medium thermal resistance; German version of EN 12939:2000.